Propagation and Radio System Design Issues in Mobile Radio Systems for the GloMo Project

Theodore S. Rappaport, Keith Blankenship, Hao Xu
Mobile and Portable Radio Research Group
Bradley Department of Electrical and Computer Engineering
Virginia Polytechnic Institute and State University
Revised January 31, 1997

This tutorial was developed for the benefit of the commercial and military wireless community working on the DARPA GloMo program and related activities, and was sponsored by DARPA/ETO under the GloMo program.

I. Introduction

An accurate quantitative understanding of the radio propagation channel is imperative for reliable wireless system design. For instance, radio propagation conditions limit the area which can be covered by a transmitter or the maximum data rate in a system. Radio propagation conditions also directly affect the battery power requirements for mobile transceivers, since receiver circuitry has a battery drain that is proportional to its complexity, and transmitter circuitry has a battery drain that is directly related to RF power output.

This tutorial introduces the reader to the fundamental concepts of propagation in mobile radio. The reader will be provided with the tools necessary to make simple link budget calculations and, given data on the time dispersive nature of the mobile radio channel, determine the maximum unequalized data rate allowed by the channel. An extensive bibliography points the reader to important papers on various topics, which can be consulted for further study.

Mobile radio propagation is usually studied in terms of large-scale effects and small-scale effects. Large-scale effects involve the variation of the mean received signal strength over large distances or long time intervals, whereas small-scale effects involve the fluctuations of the received signal strength about a local mean, where these fluctuations occur over small distances or short time intervals.

This tutorial begins in Section II by discussing the large-scale effects and presents the useful d^n model for calculating path loss. A table of typical path loss exponents, n, is provided. After introducing receiver noise, a practical *link budget* is carried out using the d^n model. Other more sophisticated models for calculating large-scale path loss are mentioned and referenced.

Section III discusses the small-scale effects in mobile radio propagation. After introducing the channel impulse response, a discussion of the various parameters used to characterize the mobile radio propagation channel is embarked upon. The various types of fading, including "fast," "slow," "flat," and "frequency selective" are defined. The time dispersive nature of the mobile radio propagation channel, which limits the maximum unequalized data rate that can be attained, will be discussed. The statistical methods for modeling the mobile radio propagation channel are mentioned and referenced, as are the various methods by which the channel parameters are measured. Section IV summarizes and concludes the tutorial.

II. Large-Scale Propagation, Battery, and Range Issues

Large-scale fading analysis is concerned with predicting the mean signal strength as a function of transmitter-receiver (T-R) separation distance (d) over T-R separations of hundreds, thousands, or millions of meters. In this section, the widely-employed and easy-to-use d^n model is presented, where d represents the T-R separation distance and relates to path loss in terms of an empirical path loss exponent, n, for whicht ypical values are tabulated. The d^n model has been shown historically to be a very good first-cut model for prediction of the distance-dependent received power in a wireless system [1]. More sophisticated models which take into account more specific information are also referenced.

A. d^n Path Loss Model- Range vs. Battery/Power Drain

The d^n path loss model is generally used to predict the power transfer between a transmitter and a receiver. This model takes into account the decrease in energy density suffered by the electromagnetic wave due to spreading, as well as the energy loss due to the interaction of the electromagnetic wave with the propagation environment. "Path loss" is the term used to quantify the difference (in dB) between the transmitted power, P_t (in dBm), and received power, P_r (in dBm). (The gains of the transmitting and receiving antennas may be implicitly included or excluded in these power quantities). The d^n model predicts that the mean path loss, $\overline{PL}(d)$, measured in dB, at a T-R separation d will be

$$\overline{PL}(d) = \overline{PL}(d_0) + 10\, n \log_{10}\left(\frac{d}{d_0}\right) \text{ (dB)} \tag{1}$$

where $\overline{PL}(d_0)$ is the mean path loss in dB at close-in reference distance d_0, and n is the empirical quantity – the "path loss exponent." Note that when $n = 2$, the path loss is the same as free space – received signals fall off by 20 dB per decade increase in distance. The reference distance, d_0, is chosen to be in the far-field of the antenna, at a distance at which the propagation can be considered to be close enough to the transmitter such that multipath and diffraction are negligible and the link is approximately that of free-space. Typically, d_0 is chosen to be 1 m for indoor environments and 100 m

or 1 km in outdoor environments. The free space distance must be in the far-field of the antenna, which is related to the physical size and frequency of the antenna. Without explicit measured information on the close-in receive distance $\overline{PL}(d_0)$, it can be measured or estimated by the following formula:

$$\overline{PL}(d_0) = 20 \log_{10} \left(\frac{4\pi d_0}{\lambda} \right) \tag{2}$$

where $\lambda = c/f$ is the wavelength of the transmitted signal (c is the speed of light, $3 * 10^8$ m/s and f is the frequency of the transmitted signal in Hz).

The path losses at different geographical locations at the same distance d (for $d > d_0$) from a fixed transmitter exhibit a natural variability due to differences in local surroundings, blockage or terrain over which the signals travel. This variabilityo ver a large number of independent measured locations the same distance away from the transmitter results in "log-normal shadowing" and is usually found to follow a Gaussian distribution (with values in dB) about the distance-dependent mean path loss, $\overline{PL}(d)$, with standard deviation σ dB about the mean path loss $\overline{PL}(d)$.

The path loss exponent, n, is an empirical constant that is often measured, but can also be derived theoretically in some environments. It varies depending upon the radio propagation environment. Table 1, taken from [1, p. 104], gives typical values for n. Typical values for the log-normal shadowing in outdoor environments range between 8 and 14 dB. Path loss exponents for indoor environments are presented in Table 2, which also presents measured values of σ.

TABLE 1

Typical Path Loss Exponents

Environment	**Path Loss Exponent,** n
Free Space	2
Urban area cellular/PCS	2.7 to 4.0
Shadowed urban cellular/PCS	3ъ5
In building line-of-sight	1.6 to 1.8
Obstructed in building	4ъ6
Obstructed in factories	2ъ3

TABLE 2

PATH LOSS EXPONENTS AND σ VALUES FOR SPECIFIC INDOOR ENVIRONMENTS.

Environment	**Freq.(MHz)**	n	σ **(dB)**	**Source**
Indoor – Retail Store	914	2.2	8.7	[2]
Indoor – Grocery Store	914	1.8	5.2	[2]
Indoor – Hard Partition Office	1500	3.0	7.0	[2]
Indoor – Soft Partition Office	900	2.4	9.6	[2]
Indoor – Soft Partition Office	1900	2.6	14.1	[2]
Indoor –F actory (LOS)	1300	1.6–2.0	3.0–5.8	[2]
Indoor –F actory (LOS)	4000	2.1	7.0	[2]
Indoor – Suburban Home	900	3.0	7.0	[2]
Indoor –F actory (Obstructed)	1300	3.3	6.8	[2]
Indoor –F actory (Obstructed)	4000	2.1	9.7	[2]
Indoor – Office Same Floor	914	2.76–3.27	5.2–12.9	[3]
Indoor – Office Entire Building	914	3.54–4.33	12.8–13.3	[3]
Indoor – Office Wing	914	2.68–4.01	4.4–8.1	[3]
Indoor –A v erage	914	3.14	16.3	[3]
Indoor – Through One Floor	914	4.19	5.1	[3]
Indoor – Through Two Floors	914	5.04	6.5	[3]
Indoor – Through Three Floors	914	5.22	6.7	[3]

Example One. Path loss calculations for free space and standard urban channels.

Evaluate the path loss at a distance of 10 km for a radio signal with a carrier frequency of 900 MHz for free space and standard urban channels.

Solution to Example One

$$\lambda = \frac{c}{f} = \frac{3 * 10^8}{9 * 10^8} = 1/3\text{m} \tag{3}$$

a) For free space propagation:

Let d_0 =1 km, n =2, then the path loss at the refence distance of 1km will be

$$\overline{PL}(d_0 = 1 \text{ km}) = 20\log_{10}\left(\frac{4\pi d_0}{\lambda}\right) = 20\log_{10}\left(\frac{4\pi 1000}{\lambda}\right) = 91.5 \text{ dB} \quad (4)$$

$$\overline{PL}(d) = \overline{PL}(d_0) + 10n\log_{10}\left(\frac{d}{d_0}\right) = 91.5 + (10)(2)\log_{10}\left(\frac{10000}{1000}\right) = 111.5 \text{ dB} \quad (5)$$

b) For standard urban:

Let $d_0 = 1$ km, $n = 4$, then the path loss will be

$$\overline{PL}(d) = \overline{PL}(d_0) + 10n\log_{10}\left(\frac{d}{d_0}\right) = 91.5 + (10)(4)\log_{10}\left(\frac{10000}{1000}\right) = 131.5 \text{ dB} \quad (6)$$

Notice that in the urban case there is 20 dB more loss over the 10 km path.

Example Two. The effect of talk time on battery life.

Assume a 1 Amp-hour battery is used on a wireless portable communications device. Assume that the radio receiver draws 35 mA on receive and 250 mA during both transmission and reception. How long would the phone work (i.e. what is the battery life), if the user has one 3-minute call every hour? What is the maximum talk time available if the transmitter is operating continuously?

Solution to Example Two

a) If the user has one 3-minute call every hour, battery lifetime T will be

$$T = \frac{1000 * 60 \text{ (mA-minute)}}{((60-3) * 35 + 3 * 250) \text{ (mA-minute)/hour}} = 21.86 \text{ hours} \quad (7)$$

b) The battery lifetime T for continuous transceiver operation is

$$T = \frac{(1000 * 60) \text{ (mA-minute)}}{250 \text{ mA}} = 240 \text{ minutes} = 4 \text{ hours} \quad (8)$$

Notice that the battery lasts at least 5 times longer when the transmitter is used for only 3 minutes per hour compared to when the transmitter is on continuously.

B. Other Models

Although extremely useful for quick estimations of link performance, the d^n model combines all propagation effects into a single parameter – the path loss exponent n. More sophisticated models have been developed to take into account other important factors that may vary from site to site, such as terrain, urban clutter, antenna heights, and diffraction. For outdoor propagation, some of the most widely used models are as follows:

- Longley-Rice ([4], [5], [6]),
- Durkin ([7], [8]),
- Okumura ([9]),
- Hata ([10]),
- COST-231 ([11]),
- Walfisch and Bertoni ([12]),
- Wideband PCS microcell ([13]).

For indoor propagation, most models in wide use rely on the basic d^n model for free space propagation, but also account for signal losses suffered in traversing each inner partition or floor. The world's first indoor propagation planning tool, SMT *Plus*, is described in [14] and provides system planning using blue prints. Similar tools for wireless planning and simulation are being developed at VAT ech as part of the DARPA GloMo project.

C. Signal Penetration into Buildings

Building penetration issues will become very important as urban wireless systems, which seek to provide ubiquitous coverage, are widely deployed. Measurements of signal penetration losses are reported in [15], [16], [17], [18], [19], and [20], which cite average penetration losses of between 7.6 and 16.4 dB into a building, depending upon building materials and frequency of operation.

D. Link Budget Calculations - Bandwidth, Power, Distance Tradeoffs

The limiting factor on a wireless link is the signal-to-noise ratio (SNR) required by the receiver for useful reception.

$$SNR = P_s/N \tag{9}$$

or when powers are measured in dBm units

$$SNR(dB) = P_s(dBm) - N(dBm) \tag{10}$$

The audio or video quality of a receiver is directly linked to the SNR; the greater the SNR, the better is the reception quality.

The power received from a transmitter at a separation distance of (d) directly impacts the SNR since the desired signal level is represented in the received power. The received power can be evaluated using the next equation:

$$P_s = P_r(d) = \frac{P_t G_t G_r}{\overline{PL}} \tag{11}$$

or when the gains are measured in dB units and the power is measured in dBm

$$P_s(dBm)=(\ P_t)_{dBm}+(\ G_t)_{dB}+(\ G_r)_{dB}-(\overline{PL}(d))_{dB} \tag{12}$$

where $P_r(d)$ is the received power in dBm, which is a function of the T-R separation distance in meters, P_t is the transmitted power in dBm,$(G_t)_{dB}$ is the gain of the transmitter antenna in dB, $(G_r)_{dB}$ is the gain of the receiver antenna in dB, and $\overline{PL}(d)_{dB}$ is the path loss of the channel in dB.

The noise might consist of thermal noise generated in the receiver, co-channel or adjacent-channel interference in frequency division or time division multiple access systems, or multiple access interference in code division multiple access spread spectrum systems. If only the thermal noise is considered, the noise power N in dBm is given by

$$N = KT_0BF \tag{13}$$

or

$$N(dBm)=\ -174\ (\text{dBm}) + 10\log_{10} B + F\ (\text{dB}) \tag{14}$$

where K =1 .38 $*\ 10^{-23}$ J/K is the Boltzmann's constant, $T_0 = 290$ K is standard temperature, B is the receiver bandwidth in Hz, and F is the noise figure of the receiver in dB (see [1, p. 565]). Typical values for F range from 5 to 10 dB for commercial receivers.

Example Three. Noise power vs. BW.

Typical values for the bandwidth in a wireless system are from 10 kHz to several MHz. If the noise figure is assumed to be 10 dB, what is the noise level at the receiver for a 30 kHz system? Plot the noise level vs. BW, where the BW is allowed to vary from 10kHz to 100 MHz.

Solution to Example Three

The noise level at the receiver is :

$$N = -174\ (\text{dBm}) + 10\log_{10} B + F\ (\text{dB}) = -174 + 10\log_{10}(30000) + 10 = -119\ \text{dBm} \tag{15}$$

The plot of noise level vs. BW is presented in Figure 1.

Example Four. Received power vs. distance for free space and a shadowed urban area.

A typical cellular subscriber unit transmits 0.6 watts of power. If the transmitter output is applied to a unity gain antenna with a 900 MHz carrier frequency, what is the received power in dBm at a

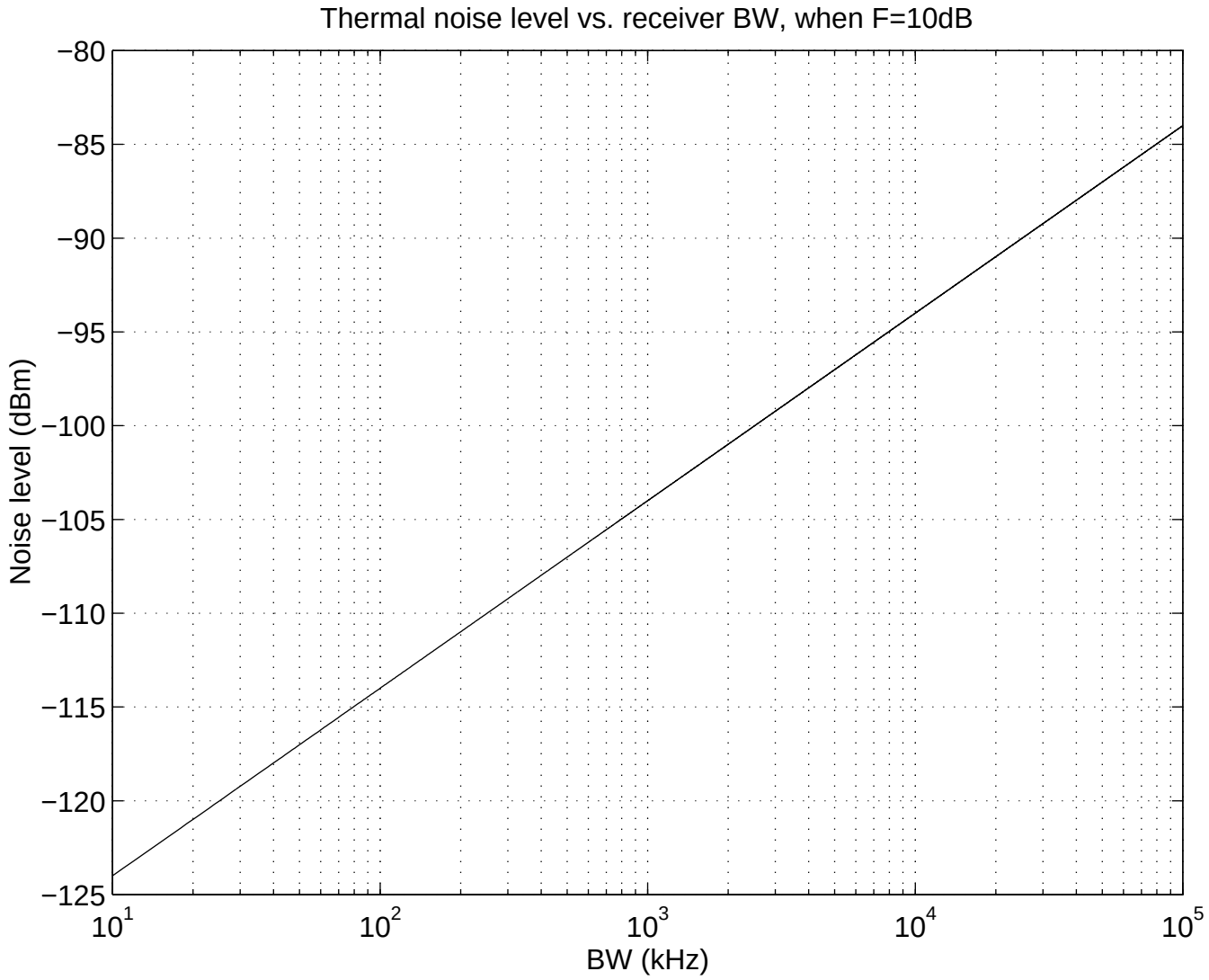

Fig. 1. Thermal noise level vs. receiver BW, when $F = 10$ dB.

free space distance of 5 km from the antenna? What is $P_r(5\text{ km})$ in a shadowed urban area where free space is assumed within 1 km from the antenna, and $n = 4$ holds for $d > 1$ km ? Plot the received power vs. distance. Assume unity gain for the receiver antenna.

Solution to Example Four

Given:

Transmitter power, $P_t = 0.6$ W. Carrier frequency, $f_c = 900$ MHz.

The wave length and path loss can be determined as:

$$\lambda = \frac{c}{f} = 3 * 10^8/(9 * 10^8) = 1/3 \text{ m} \tag{16}$$

$$\overline{PL}(d_0) = \frac{(4\pi)^2 {d_0}^2}{\lambda^2} = \frac{(4\pi)^2 1000^2}{(1/3)^2} = 1.42 * 10^9 = 91.53 \text{ dB} \tag{17}$$

a) For free space $n = 2$, at $d = 5km$

$$\overline{PL}(d) = \overline{PL}(d_0) + 10n \log_{10}\left(\frac{d}{d_0}\right) = 91.53 + (10)(2)\log_{10}\left(\frac{5000}{1000}\right) = 105.53 \text{ dB} = 105.5 \text{ dB} \tag{18}$$

$$P_r = (P_t)_{dBm} + (G_t)_{dB} + (G_r)_{dB} - (\overline{PL}(d))_{dB} = 27.8 + 0 + 0 - 105.5 = -77.7 \text{ dBm} \tag{19}$$

where the antenna gains are 0 dB.

b) For a shadowed urban area where $n = 4$, at $d = 5$ km the path loss and the received power will be:

$$\overline{PL}(d) = \overline{PL}(d_0) + 10n \log_{10}\left(\frac{d}{d_0}\right) = 91.53 + (10)(4)\log_{10}\left(\frac{5000}{1000}\right) = 119.5 \text{ dB} \tag{20}$$

$$P_r = (P_t)_{dB} + (G_t)_{dB} + (G_r)_{dB} - (\overline{PL}(d))_{dB} = 27.8 + 0 + 0 - 119.5 = -91.7 \text{ dBm} \tag{21}$$

c) The plot of received power vs. separation distance is shown in Figure 2. Notice that, as the distance increases, the signal becomes markedly weaker in the urban environment.

Example Five. Maximum separation distance vs. transmitted power (with fixed BW).

In Example Four, if the signal to noise ratio is required to be at least 25 dB for the receiver to properly distinguish the signal from noise, what will be the maximum separation distance? Assume the receiver has BW of $B = 30$ kHz and noise figure of $F = 10$ dB. If the transmitted power is allowed to vary from 0.1 W to 3 W, plot the maximum separation distance vs. the transmitted power.

Solution to Example Five

If the receiver has a BW of $B = 30$ kHz and a noise figure of $F = 10$ dB, then the noise level will be $N = -119$ dBm (See Example Three). A required SNR of 25 dB means that the received signal power, P_r, must be such that $P_r > (-119 + 25)$ dBm or $P_r > -94$ dBm. Assuming that the transmitted signal power is 0.6 W, or 27.78 dBm, this allows a path loss of up to $\overline{PL} = P_t - P_r$, or 122 dB.

Assuming an outdoor cellular environment using a reference distance d_0 of 1 km and an operating frequency of 900 MHz ($\lambda = 1/3$ m), the path loss at the reference distance, $\overline{PL}(d_0) = 91.5$dB (See Example Four).

a) For free space channel:

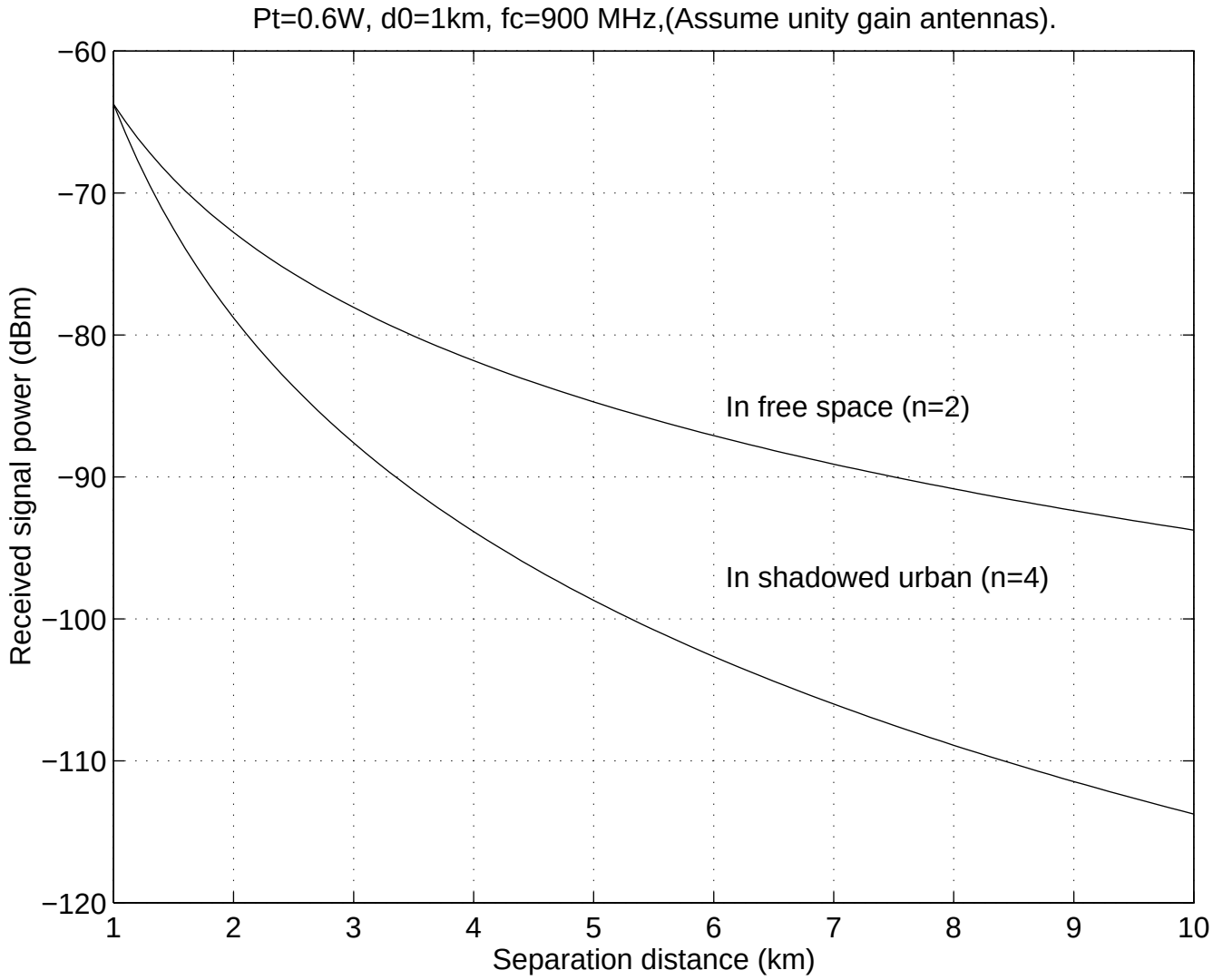

Fig. 2. Received power vs. separation distance, when $P_t = 0.6$ W, $d_0 = 1$ km, $f_c = 900$ MHz, $n = 4$.(Assume unity gain antennas at both ends).

The path loss exponent is 2 in free space, so the d^n path loss model predicts that a path loss of 122 dB occurs at

$$122 = 91.5 + 10(2)\log_{10}\left(\frac{d}{1\text{ km}}\right) \tag{22}$$

Solving for d, we find $d = 33.5$ km. Thus, the link could operate at SNR of 25 dB or greater for T-R separations of up to 33.5 km in free space.

b) For a shadowed urban channel:

Assuming a path loss exponent of 4, typical for a shadowed urban area cellular radio, the d^n path loss

model predicts that a path loss of 117 dB occurs at

$$122 = 91.5 + 10(4)\log_{10}\left(\frac{d}{1\text{ km}}\right) \tag{23}$$

or $d = 5.8$ km. Thus, the link could operate at SNR of 25 dB or greater for T-R separations of up to 5.8 km in a typical shadowed urban area.

c) The plot of maximum separation distance vs. the transmitted power is shown in Figure 3. Notice that for the same amount of transmitted power, the maximum separation distance decreases by a factor of its square root in the urban environment as compared to the free space environment.

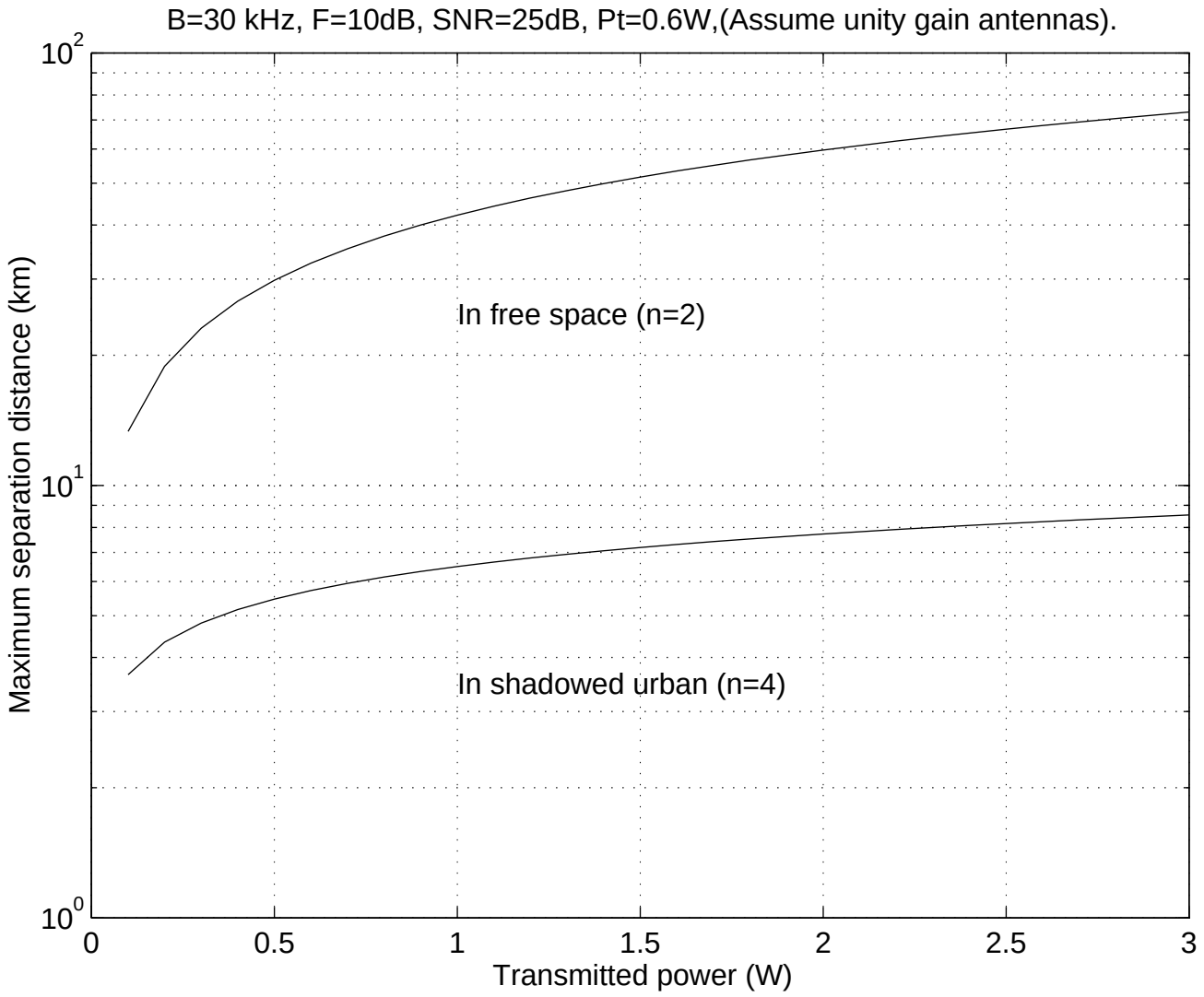

Fig. 3. Maximum separation distance vs. transmitted power, when $B = 30$ kHz, $F = 10$ dB, $SNR = 25$ dB, $P_t = 0.6$ W.(Assume unity gain antennas at both ends).

Example Six. Maximum BW vs. transmitted power (with fixed separa-

tion distance).

If a maximum separation distance of 5 km is required and if the transmitted power is 0.6 W, what is the maximum BW allowed for a mobile communication system operating over free space? Assume a 10 dB receiver noise figure and a required SNR of 25 dB. If the transmitted power is allowed to vary from 0.1 W to 3 W, plot the maximum BW vs. transmitted power. Assume unity gain antennas at both ends.

Solution to Example Six

a) From Example Four we know that the pass loss is: $\overline{PL}(d) = 105.5$ dB at a distance of $d = 5km$ for a free space channel. The received power is:

$$P_r = (P_t)_{dBm} + (G_t)_{dB} + (G_r)_{dB} - (\overline{PL}(d))_{dB} = 27.8 + 0 + 0 - 105.5 = -77.7 \text{ dBm} \tag{24}$$

Assuming that the signal to noise ratio must be 25 dB, then the maximum noise power should be $N = -77.7 - 25 = -102.7$ dB. From

$$N = -174 \text{ dBm} + 10 \log_{10} B + F \text{ (dB)} = -174 + 10 \log_{10}(B) + 10 = -102.7 \text{ dBm} \tag{25}$$

Solving for B, we find

$$B = 1.349MHz \tag{26}$$

b) For a shadowed urban area, let $d = 5$ km, $n = 4$, the path loss will be:

$$\overline{PL}(d) = 119.5 \text{ dB} \tag{27}$$

The received power is:

$$P_r = (P_t)_{dB} + (G_t)_{dB} + (G_r)_{dB} - (\overline{PL}(d))_{dB} = 27.78 + 0 + 0 - 119.5 = -91.7 \text{ dBm} \tag{28}$$

The maximum noise level should be $N = -116.7$ dBm for $SNR = 25$ dB, and solving for B, we find

$$N = -174 \text{ dBm} + 10 \log_{10} B + F \text{ (dB)} = -174 + 10 \log_{10}(B) + 10 = -116.7 \text{ dBm} \tag{29}$$

$$B = 53.7 \text{ kHz}. \tag{30}$$

Notice that in the urban environment the channel bandwidth is 20 times smaller than that in a free space channel for the same quality of reception on the 5 km link.

c) The plot of maximum BW vs. transmitted power is shown in Figure 4.

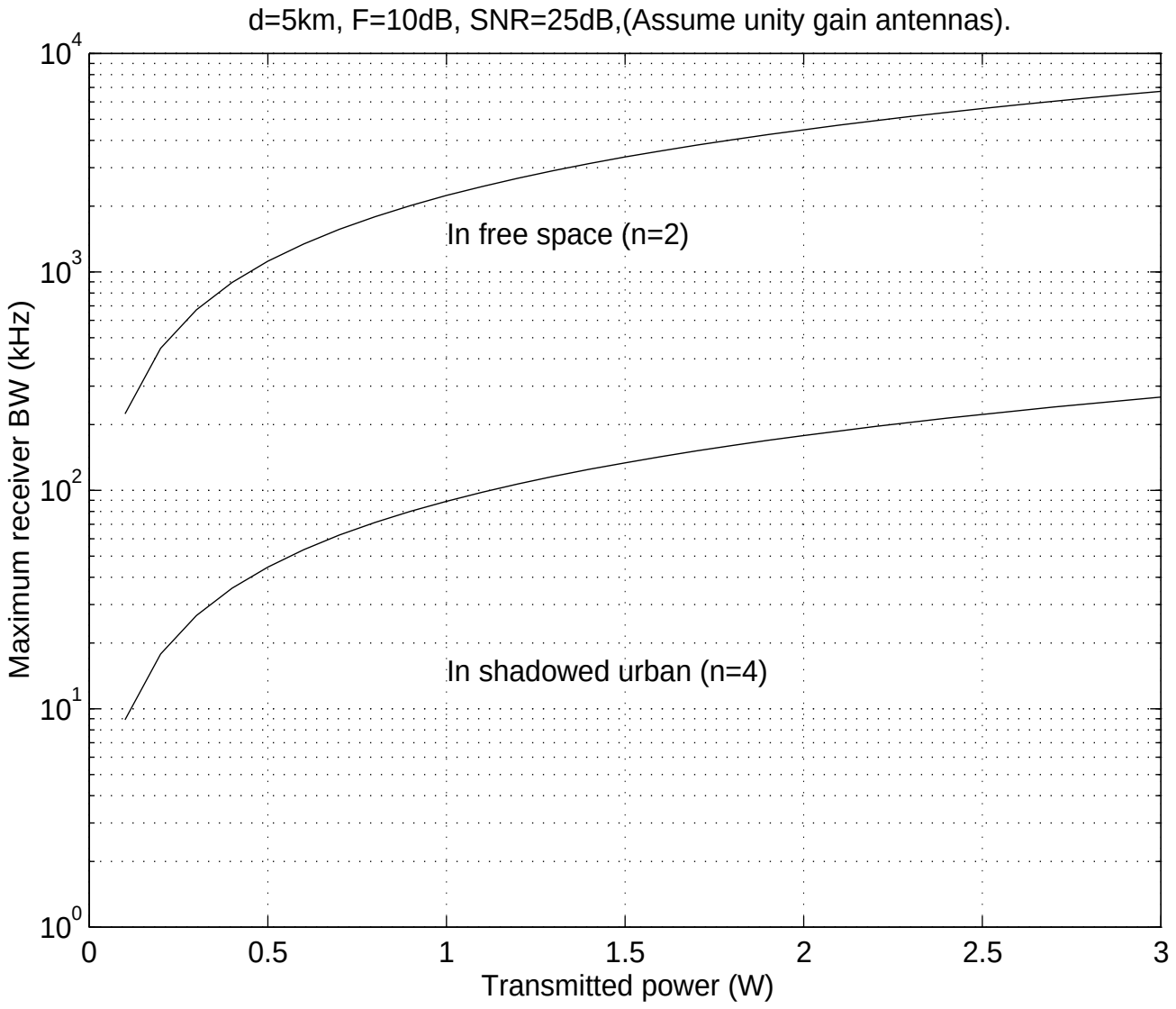

Fig. 4. Maximum BW vs. transmitted power, when $d = 5$ km, $F = 10$ dB, $SNR = 25$ dB, $n = 4$.(Assume unity gain antennas at both ends).

E. Choice of Modulation and its Effect on Efficiency

Various modulation techniques are used in mobile communication systems. In the first generation mobile radio systems, analog modulation schemes are employed. Since digital modulation offers numerous benefits, it is being used to replace conventional analog systems.

The most popular analog modulation technique used in mobile radio systems is frequency modulation (FM). FM offers many advantages over amplitude modulation (AM). FM has better noise immunity and superior qualitative performance in fading when compared to amplitude modulation because the information in FM signals is represented as frequency variations rather than as amplitude variations.

In FM systems it is possible to tradeoff bandwidth occupancy for improved noise performance by varying the modulation index(i.e. the RF bandwidth). FM is more power efficient than AM. Since an FM signal is a constant envelope signal, the transmitted power of an FM signal is constant regardless of the amplitude of the message signal. This allows Class C power amplifiers, which have power efficiencies on the order of 70%, to be used for RF power amplification. In AM, however, linear Class A or AB amplifiers, which have power efficiencies of $30-40\%$, must be used to maintain the linearity between the applied message and the amplitude of the transmitted signal. Some of the disadvantages of the FM systems are inefficiency in bandwidth, complexity of the receiver and transmitter, and the requirement that the received signal power must be above a threshold for correct detection, etc. [1, p.198]

Modern mobile communication systems use digital modulation techniques. Digital modulation has many advantages over analog modulation. Some advantages include greater noise immunity and robustness to channel impairments, easier multiplexing of various forms of information (e.g. voice, data, and video), and greater security. Several factors influence the choice of a digital modulation scheme. A desirable modulation scheme provides low bit error rates at low received signal-to-noise ratios, performs well in multipath and fading conditions, occupies a minimum of bandwidth, and is easy and cost-effective to implement. Existing modulation schemes do not simultaneously satisfy all of these requirements. Some are better in terms of the bit error rate performance, while others are better in terms of bandwidth efficiency. Depending on the demands of the particular application, trade-offs are made when selecting a digital modulation. For example, higher level modulation schemes (M-ary keying) decrease bandwidth occupancy but increase the required received power, and hence trade power efficiency for bandwidth efficiency. In general, the modulation, interference, and implementation of the time-varying effects of the channel as well as the performance of the specific demodulator are analyzed as a complete system using simulation to determine relative performance and ultimate selection. [1, p.220]

Example Seven. Battery life vs. transmitted power.

If a 1 Amp-hour battery is used for a mobile wireless terminal, and the continuous transmitted power of the terminal is 0.6 W, what is the battery life? Plot the battery life vs. transmitted power, if the transmitted power is allowed to vary from 0.1W to 3 W. Assume the power supply voltage is 12 V, and the transmitted power is 60% of the overall power consumed by the terminal.

Solution of Example Seven

The consumed power of the subscriber unit is $0.6/60\% = 1$ W, and the consumed current is $1\text{ W}/12\text{ V} =$

0.0833 amp. The lifetime of the battery is 1 Amp-hour/0.0833 amp = 12 hour.

The plot of the battery life vs. transmitted power is shown in Figure 5. This curve shows the important relationship between talk time and transmitted power. Notice that in the example we used 60% power efficiency, considering a 70% power efficiency for the Class C amplifier and some efficiency loss in the rest of the circuitry.

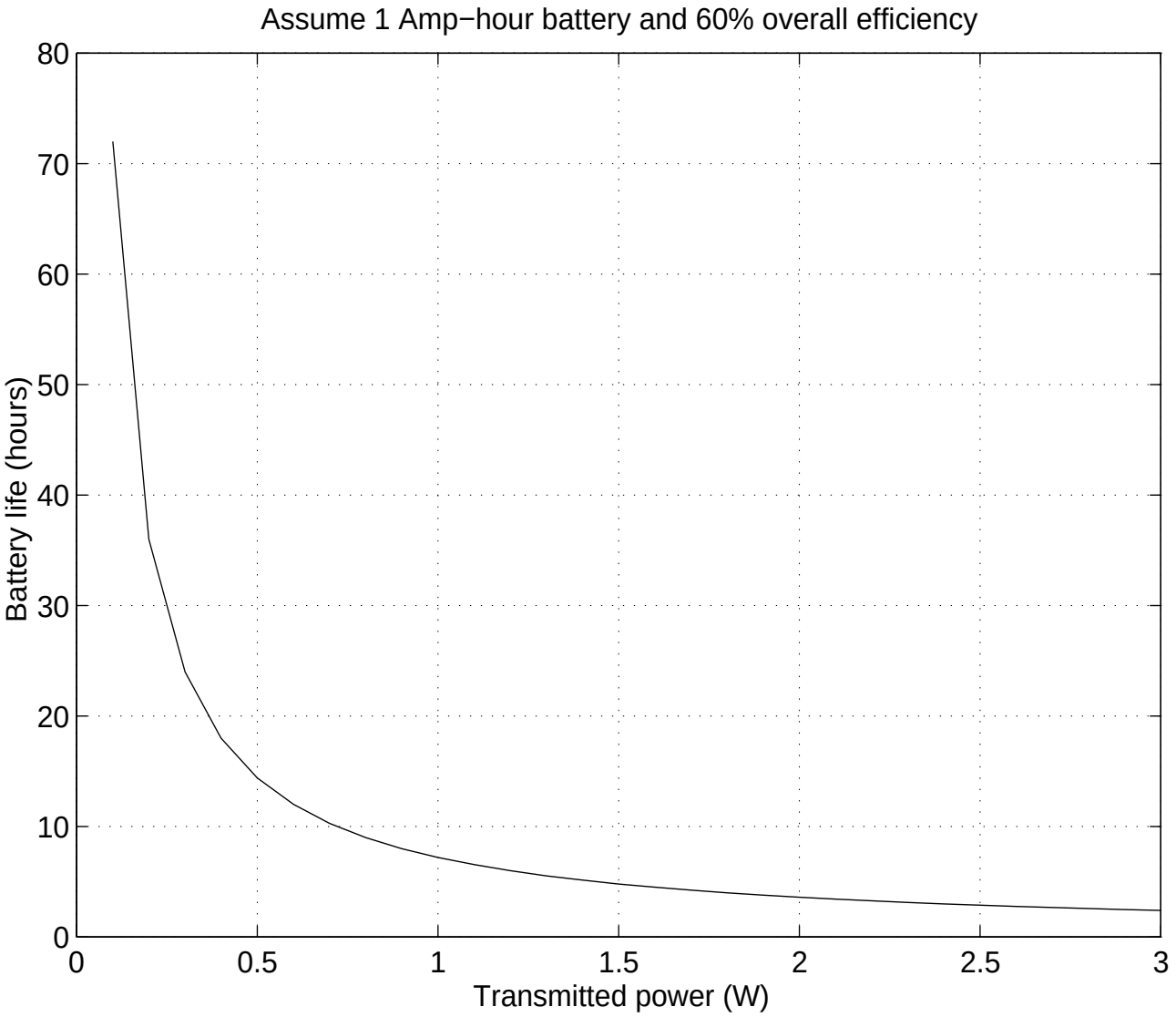

Fig. 5. The battery life vs. transmitted power, when using 1 Amp-hour battery and assuming 60% overall efficiency.

A combined plot of the maximum separation distance and battery life vs. transmitted power is shown in Figure 6. The combined plot of the maximum BW and battery life vs. transmitted power is shown in Figure 7. These plots show the relationship among the maximum separation distance, maximum

bandwidth, transmitted power and battery life. The plots can be used to design the propagation system or tradeoff the maximum separation distance and the maximum bandwidth against the battery life. For instance, when the bandwidth is given to be 30 kHz, from Figure 6, one can tradeoff the maximum separation distance against battery lifetime by varying the transmitted power. If we change the transmitted power from $W = 0.6W$ to $W = 1W$, then from the plot we can find that the value of the battery life decreases approximately from $t = 12$ hours to $t = 9$ hours, while the maximum separation distance in standard urban increases from $d = 5.5$ km to $d = 6.5$ km . Similar estimation can be undertaken for the tradeoff of the maximum bandwidth against the battery life using Figure 7, where the maximum separation distance is known to be 5 km. In Figures 6 and 7 we assumed 60% overall power efficiency as we did in Example Seven.

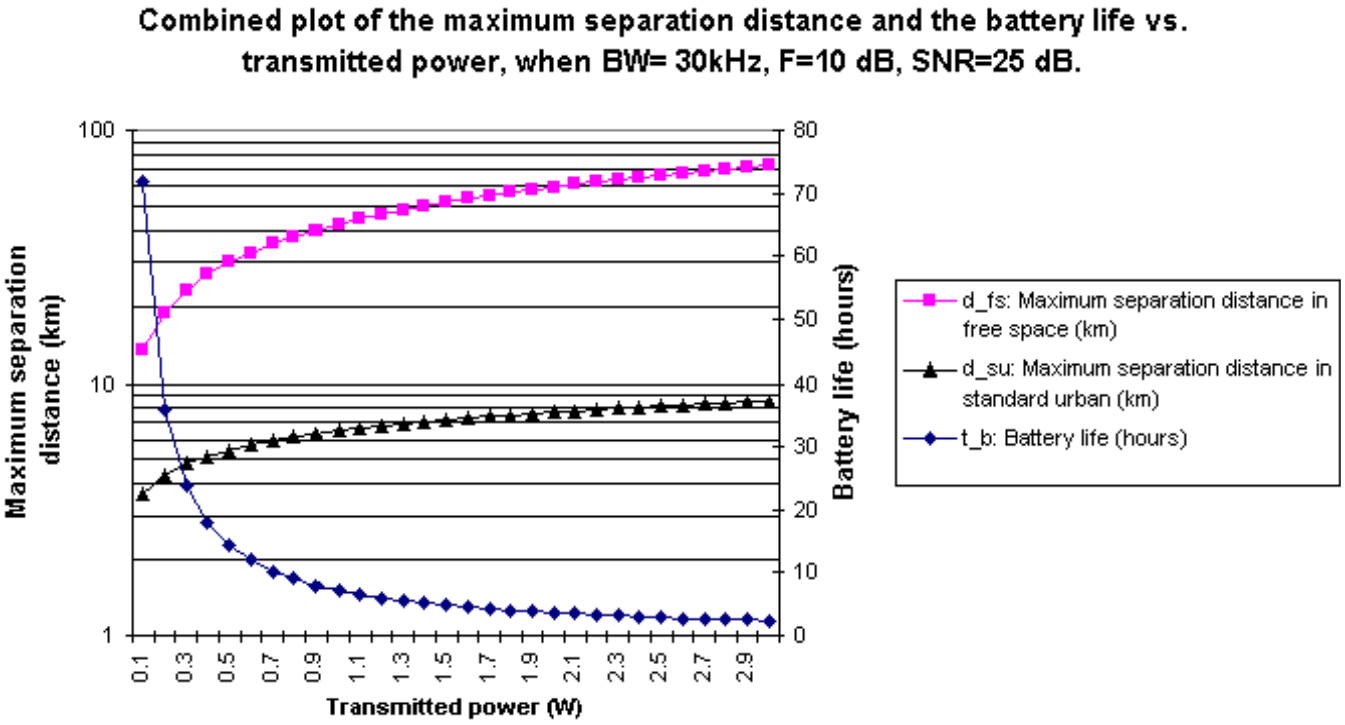

Fig. 6. Separation distance and battery life vs. transmitted power.(Assume unity gain antennas and 60% efficiency).

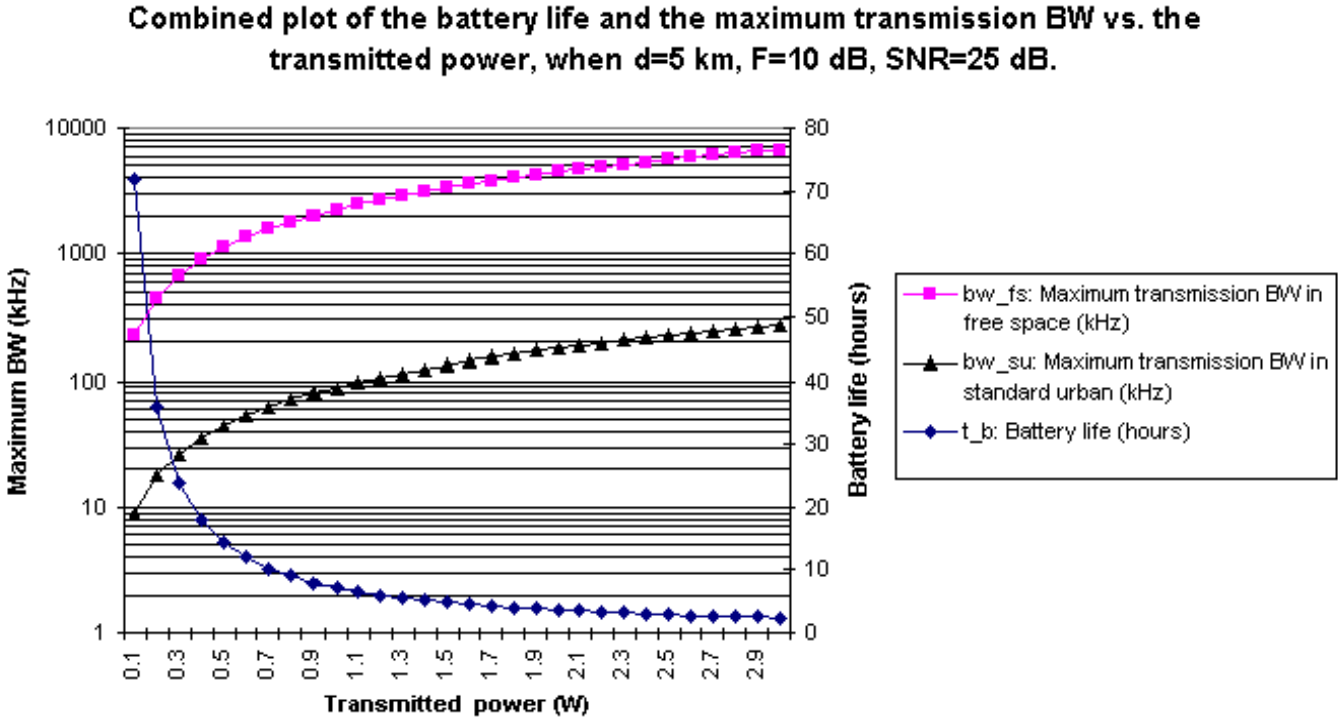

Fig. 7. BW and battery life vs. transmitted power.(Assume unity gain antennas and 60% efficiency).

III. Small-Scale Fading

Whereas in large-scale propagation the average local signal strength is studied over large spatial distances, small-scale fading is concerned with the more rapid fluctuations of the signal over short time periods or over short distances. Multiple versions of the signal arrive at the receiver at different times and are subjected to constructive and destructive interference, which results in fading. Fading manifests itself in three main ways [1, p. 139]: (1) variation of the signal strength over short distances or short time intervals, (2) undesired frequency modulation on the signal due to Doppler shifts, and (3) time dispersion due to multipath propagation delays.

In this section, the channel impulse response is first presented. Various useful gross-level parameters which have been developed to characterize the channel are presented next, followed by a discussion of the types of small-scale fading which can occur. The models that have been developed to simulate small-scale fading are useful for system design and simulation and are mentioned. The section concludes with a description of the methods used to obtain real-world data on the small-scale characteristics of a wireless channel.

A. Impulse Response

In mobile radio, signal propagation between the transmitter and receiver can be conceptualized by introducing the concept of the mobile radio channel impulse response, which introduces a filtering action on the signal. The channel impulse response is assumed to be time-invariant (which is usually not the case in mobile radio). The baseband impulse response, $h(t)$, can be expressed as

$$h(t) = \sum_{i=1}^{N} a_i e^{\theta_i} \delta(t - \tau_i) \tag{31}$$

where a_i is the voltage amplitude of the i^{th} arriving signal, θ_i is the phase shift of the i^{th} arriving signal, and τ_i is the time delay of the i^{th} arriving signal. This shows that, in general, the received signal is a series of time-delayed, phase-shifted, attenuated versions of the transmitted signal. If the channel is not time-invariant, then a_i, θ_i, and τ_i are also functions of time. The parameters of $h(t)$ can be directly measured using wideband channel sounding techniques (see Section III-E). The parameters may be used to create realistic small scale models of the propagation channel for system design and simulation. Software packages such as SIRCIM [21] and SMRCIM [22] use this concept.

B. Parameters of the Mobile Radio Channel

In order to characterize the mobile radio channel, several parameters have been developed which provide insight into the effect of the channel upon the transmitted signal. The most important of these are the RMS delay spread, the coherence bandwidth, and the coherence time of the channel.

TABLE 3

Typical RMS delay spreads in various environments.

Environment	**Freq. (MHz)**	σ_τ **(ns)**	**Notes**	**Source**
Urban – New York City	910	1300	Average	[23]
Urban – New York City	910	600	Standard Deviation	[23]
Urban – New York City	910	3500	Maximum	[23]
Urban – San Francisco	892	1000–2500	Worst Case	[24]
Suburban	910	200–310	Averaged Typical Case	[23]
Suburban	910	1960–2110	Averaged Extreme Case	[23]
Indoor – Office Building	1500	10–50		[25]
Indoor – Office Building	1500	25	Median	[25]
Indoor – Office Building	850	270	Maximum	[26]
Indoor – Office Buildings	1900	70–94	Average	[27]
Indoor – Office Buildings	1900	1470	Maximum	[27]

The RMS delay spread of a mobile radio channel characterizes the time dispersive nature of the channel. The RMS delay spread, σ_τ, is found from the impulse response function of the channel according to the formula

$$\sigma_\tau = \sqrt{\overline{\tau^2} - (\overline{\tau})^2} \tag{32}$$

where

$$\overline{\tau} = \frac{\sum_k a_k^2 \tau_k}{\sum_k a_k^2} \tag{33}$$

(often referred to as the mean excess delay), and

$$\overline{\tau^2} = \frac{\sum_k a_k^2 \tau_k^2}{\sum_k a_k^2} \tag{34}$$

where a_k is the voltage amplitude of the k^{th} multipath component and τ_k is the delay of the k^{th} multipath component. Table 3 provides some typical values for σ_τ. The value of σ_τ describes the time delay spread in a multipath channel, beyond what would be expected for free space line-of-sight transmission.

Coherence bandwidth is a statistical measure of the range of the frequencies over which the channel can be considered "flat" (i.e., a channel which passes all spectral components with approximately equal

gain and linear phase). In other words, coherence bandwidth is the range of frequencies over which two frequency components have a strong potential for amplitude correlation [1]. In [28], it is shown that if any two arbitrary spectral components over the bandwidth B_c exhibit a cross-correlation greater than 0.9, then B_c is related to the RMS delay spread according to the approximate formula

$$B_c \approx \frac{1}{50\sigma_\tau} \tag{35}$$

Similarly, if the cross-correlation of any two spectral components is reduced to 0.5, then B_c is related to the RMS delay spread according to the approximate formula

$$B_c \approx \frac{1}{5\sigma_\tau} \tag{36}$$

While approximate, the essence of these two equations is that the coherence bandwidth bears an inverse relationship to the RMS delay spread, σ_τ.

Relative motion between the transmitter and receiver impresses a Doppler shift upon the frequency of the transmitted signal, which means that the received signal will be a frequency shifted version of the transmitted signal. The frequency shift, f_d, is given by $f_d = (v/\lambda)cos\theta$, where v is the magnitude of the relative velocity between the transmitter and receiver and λ is the wavelength of the transmitted signal. The angle θ describes the angle of the received signal in relation to the direction of motion. In mobile radio, where the relative transmitter-receiver velocity varies with time, f_d will also vary with time, thus the frequency of the received signal will appear to vary with time. As a result, the Doppler shift tends to introduce a FM modulation into the signal. For instance, a continuous-wave (CW) signal of frequency f_c, which is transmitted over a mobile radio channel, will spread out over the bandwidth $f_c \pm f_m$, where $f_m = max(f_d)$ is the maximum Doppler shift suffered by the signal. The direction of arrival of energy determines the exact Doppler shift.

The coherence time of a mobile radio channel is the time over which the channel impulse response can be considered stationary, thus the same signal received at different points in time is likely to be highly correlated in amplitude. As a rule of thumb (see [1, p. 164]), the coherence time, T_c, is inversely proportional to the maximum Doppler shift suffered by the signal, f_m, according to the formula

$$T_c = \frac{0.423}{f_m} \tag{37}$$

C. Types of Fading

There are two types of fading due to time dispersion, and two types of fading due to Doppler spread. Time dispersion is due to the multipath delays in the channel, and has nothing to do with the motion of a mobile or the channel. Doppler spread has to do with the motion of the mobile or the channel, and has nothing to do with the multipath time delay spread of the channel.

To describe fading due to time dispersion, the terms "flat" and "frequency selective" are used. "Flat" implies that the channel has a constant amplitude response and linear phase response over a bandwidth which is greater than the bandwidth of the transmitted signal. In the time domain, this implies that the channel impulse response is like a delta function as compared to the signal modulation symbol duration. "Frequency selective" implies that the channel possesses a constant gain and linear phase response over a bandwidth which is smaller than the bandwidth of the transmitted signal. And in the time domain, the impulse response of the channel has a time duration that is equal to or greater than the width of the modulation signal. That is, when the channel time dispersion is greater than the time it takes to send the signal, the channel has memory and induces distortion that can only be undone by an equalizer. This is why high data rate digital mobile radio standards like GSM and IS-136 require an equalizer, while older, lower data rate mobile systems like AMPS do not require an equalizer.

The data rate which can be supported by a radio channel is a function of the multipath delays which occur due to reflection and diffraction in the radio channel, as well as the complexity of the receiver. In simple receivers, where an equalization circuit is not used, the maximum data rate R (bits/second) that may be supported by the channel is inversely proportional to the RMS delay spread that exists in the channel. The effects of the time delay spread on portable radio communications channels with digital modulation were studied extensively by Chuang in [29], Glance and Greenstein in [30], and Thoma, Fung and Rappaport in [31]. For nonequalized channels, the maximum data rate which may be sent before the time dispersion produces significant errors from intersymbol interference into channel is related to the RMS delay spread σ_τ by

$$max(R_b) = \frac{d}{\sigma_\tau} \tag{38}$$

where factor d is dependent on the specific channel, interference level, and modulation type being used. A common rule-of-thumb based on the extensive work in [29], [30] and [31] is that when the RMS delay spread of the channel, σ_τ, exceeds one-tenth of the data rate of the transmitted signal, an equalizer is required to mitigate the time-dispersive effects introduced by the channel. Thus, for $d = 0.1$, the maximum data rate through a channel without equalization is

$$max(R_b) = \frac{0.1}{\sigma_\tau} \tag{39}$$

When the receiver uses an equalizer, it is possible to transmit data rates that greatly exceed the inverse of the RMS delay spread. In such a case, the update rate of the equalizer is dependent on the rate of change of the channel in time, which is described by the Doppler spread. The Doppler spread describes the time rate of change of the state of the channel. For example, if a channel has a 100 Hz

Doppler spread, then the radio channel changes its "state" at a rate of 100 times per second, and a particular trained state of an equalizer may be assumed to be static for 1/100 or 0.01 seconds. The Doppler spread, when used to describe the "staticness" or short term "stationarity" of the channel, yields insight into the proper length for block codes that may be used to protect data on a wireless link.

Example Eight. Nonequalized data rates for different environments.

Using the data in Table 3 calculate the maximum unequalized data rates for different environments. Assume $d = 0.1$.

Solution to Example Eight

For nonequalized channels, the maximum data rate is given by:

$$max(R_b) = \frac{d}{\sigma_\tau} \tag{40}$$

For Urban-New York City, $\sigma_\tau = 1300(ns)$

$$max(R_b) = \frac{d}{\sigma_\tau} = \frac{0.1}{1300 * 10^{-9}} = 76,923 \text{ bps} = 76.9 \text{ kbps} \tag{41}$$

For suburban, $\sigma_\tau = 200(ns)$

$$max(R_b) = \frac{d}{\sigma_\tau} = \frac{0.1}{200 * 10^{-9}} = 500,000 \text{ bps} = 500 \text{ kbps} \tag{42}$$

For indoor office building, $\sigma_\tau = 70(ns)$

$$max(R_b) = \frac{d}{\sigma_\tau} = \frac{0.1}{70 * 10^{-9}} = 1.429 \text{ Mbps} \tag{43}$$

Notice how a small value of σ_τ yields a larger bit rate. Of course, equalization may be used to increase data rates at the expense of more complexity and power drain.

"Fast" and "slow" fading relate the coherence time of the channel, T_c, to the symbol period of the transmitted signal, T_s. Fast fading occurs when $T_c < T_s$; therefore, the channel changes faster than the transmitted signal. On the other hand, slow fading occurs when $T_c > T_s$; therefore, the channel changes slower than the transmitted signal. Generally speaking, in today's mobile radio, the fading is almost always slow, since Doppler spreads are usually less than 100 Hz, whereas symbol rates are on the order of 30 kHz or more.

The envelopes of signals in flat fading channels can often be described as being distributed according to either Rayleigh or Ricean distributions. The Rayleigh distribution describes the distribution of the envelope about its RMS value when the line-of-sight between the transmitter and receiver is obstructed.

The Rayleigh distribution describes the envelope because, due to the arrival of numerous out-of-phase multipath components, the in-phase (I) and quadrature (Q) components of the signal are Gaussian in nature. Hence, the signal envelope, which is the square root of the sum of the squares of the I and Q signals, follows a Rayleigh distribution. The Ricean distribution, on the other hand, describes the envelope of the signal when there is a dominant line-of-sight component in the received signal. As the dominant signal becomes weak, the Ricean distribution degenerates into a Rayleigh distribution.

D. Models for Small-Scale Propagation Phenomena

For detailed wireless systems design, the small-scale effects in the mobile radio channel are often simulated, and a simulated transmitted signal is subjected to the effects of the simulated channel. Demodulation of the corrupted signal at the receiver may result in bit errors. The amount of the distortion the channel has upon the signal will directly inpact the quality of the demodulated signal. In some channel models, an impulse response is generated, with which the transmitted bit stream can be convolved to obtain the received signal. Generally speaking, the models are statistical in nature, representing typical channels in various propagation environments. However, progress is being made into ray tracing and other methods which use site-specific information to derive the channel impulse response function for specific geographical regions. It should be noted that small-scale simulation is vital for synchronization, equalization, error control coding, or diversity design in practical wireless systems.

Clarke [32] and Gans [33] developed methods by which the Rayleigh fading envelope can be simulated. The added complexity of multipath time delay is rectified in such models as the two-ray Rayleigh fading model [1, p. 188] which builds upon the model of Clarke and Gans. Software packages such as SIRCIM [21] and SMRCIM [22] are statistical in nature, based on measured data. These programs generate channel impulse responses for typical propagation environments based upon environmental factors and mobile velocity. Recently, models have been introduced to statistically model the angle-of-arrival of the received signal ([34], [35]). Such models are needed for research into adaptive arrays for mobile communications.

E. Measurements of Small-Scale Propagation Phenomena

The small-scale phenomena of flat fading channels can be measured with narrowband CW signals. However, in order to measure the time dispersive effects in small-scale propagation as discussed above, wideband techniques are required. Historically, three wideband techniques have been used [1, pp.153–159]. These include the following:

- the *swept frequency technique*, in which a network analyzer is used to sweep a frequency range, measuring the s-parameter, s_{21}, over the bandwidth. The measurement can be converted to the time domain by means of a fast Fourier transform. This method suffers from the fact that the time required to sweep the channel is often much longer than the coherence time T_c.
- *pulsed techniques*, in which a pulse train with inter-pulse times greater than the maximum measurable channel delay is transmitted. The echoes of the received pulses are recorded by the receiver. The measure of the channel impulse response is determined from the strength and time delays of the pulses. This method suffers from the need for wideband RF filtering, and therefore the dynamic range is limited.
- *spread spectrum sliding correlator techniques*, in which a spread spectrum signal is transmitted. The receiver's pseudonoise (PN) clock runs at a slightly slower rate than the PN clock rate of the transmitted signal. This allows the receiver's PN code to gradually slide relative to the transmitted PN code and to eventually become correlated with all multipath components in the channel. The method benefits from the ability to use narrowband processing, thus rejecting much of the passband noise otherwise admitted by the pulsed techniques.

Recently, there has been growing interest in measurements at higher frequencies, including the 28 GHz, 37.2 GHz, and 60 GHz frequency bands. References [36] through [50] contain literature on higher frequency measurements.

F. Impact of Antenna Gain and Fading

As discussed in section III-C, in a radio communication system, multipath can limit performance either by introducing fading in narrowband systems or causing intersymbol interference in wideband systems [51]. One way to mitigate the effect of multipath interference is to use the spatial filtering technique. The basic idea of spatial filtering is to use directional antennas instead of omnidirectional antennas to emphasize signals received from one direction and attenuate signals from other directions. Spatial filtering can be employed in one of three forms: sectorized systems, switched beam systems, or adaptive antennas.

- In *sectorized systems*, the cell is divided into three or six angular regions. The base station typically uses directional antennas with 60 or 120 degree beamwidths to cover these regions. The system capacity is increased due to the decrease of the amount of the co-channel interference from the other users within its own channel. The proposed IS-95 CDMA standard incorporates a degree of spatial processing through the use of simple sectored antennas at the cell site. It employs three 120 degree wide receive and transmit beams to cover the azimuth. Sectoring nearly triples system

capacity in CDMA.[52]

- In *switched beam systems*, each sector in a cell is divided into smaller angular regions, each of which is covered by a narrow beamwidth antenna. A simple switched beam technique is to select the antenna which provides the best signal for a particular mobile unit[53].
- In *adaptive antenna systems*, a steerable adaptive antenna is used on the base station receiver. The adaptive array is capable of steering a directional antenna beam in order to maximize the signals from a desired user while attenuating signals from the other users. Systems which form a different beam for each user using switched beam or adaptive antenna technology are also referred to as intelligent antennas or smart antennas.[53]

A list of references is included for the further study of spatial filtering. Some of the recent work at MPRG in this area is presented in [34], [35] and [54], including the analysis of CDMA cellular systems employing adaptive antennas in multipath environments, descriptions of the geometrically based statistical channel model for macrocellular mobile environments and geometrically based model for light-of-sight multipath radio channels. For example, [35] uses the geometrically based single bounce macrocell (GBSBM) channel model to analyze multipath and fading. When the antenna beamwidth is narrowed, the radius of the scattering circle is decreased. With a decrease in the radius of the scattering circle, the GBSBM model predicts that the range of angles of arrival of multipath components and the Doppler spread will both decrease. Consequently, the fading will be reduced. The plot of the fading envelopes with scattering circles of different radii is presented in [35].

IV. Summary and Conclusion

This tutorial has given the reader a brief introduction to the concepts relevant to the mobile radio propagation channel and practical system design, bandwidth, and power issues. Large-scale effects were dealt with in Section II, focusing on the widely-used d^n path loss model. An example of the use of this model was given Section II-D. The reader is encouraged to employ the list of typical path loss exponents in Table 1 for quick link budget calculations. Section III dealt with the small-scale effects in mobile radio propagation. The parameters which characterize the mobile radio propagation channel – σ_τ, B_c, and T_c – were introduced. The relation of these parameters to those of the transmitted signal determine the type of fading the signal experiences and some important aspects of wireless communication system design, including whether or not an equalization stage is required in the receiver. Some of the statistical methods for modeling the mobile radio propagation were touched upon, before the tutorial concluded with a cursory description of the techniques by which the parameters of the mobile radio propagation channel are measured in practice. The extensive bibliography should provide

the reader with a starting point by which to explore the topics covered in this tutorial in greater depth.

V. Acknowledgement

Thanks to Rob Ruth and Ken Gabriel of DARPA, and Jim Schaffner at Hughes, who are program managers supporting our propagation work. Special thanks to Richard Roy of ArrayComm and Bruce Fette of Motorola who have provided suggestions for improvement for this document.

References

[1] T. S. Rappaport, *Wireless Communications: Principles and Practice*, Prentice Hall PTR, Upper Saddle River, New Jersey, 1996.

[2] J. B. Anderson, T. S. Rappaport, and S. Yoshida, "Propagation Measurements and Models for Wireless Communications Channels," *IEEE Communications Magazine*, November 1994.

[3] S. Y. Seidel and T. S. Rappaport, "914 MHz Path Loss Prediction Models for Indoor Wireless Communications in Multifloored Buildings," *IEEE Transactions on Vehicular Technology*, vol. 40, no. 2, pp. 207–217, February 1992.

[4] A. G. Longley and P. L. Rice, "Prediction of tropospheric radio transmission loss over irregular terrain," Tech. Rep. ERL 79-ITS 67, ESSA Technical Report, 1968.

[5] P. L. Rice, A. G. Longley, K. A. Norton, and A. P. Barsis, "Transmission loss predictions for tropospheric communication circuits," Tech. Rep., NBS Tech Note 101, issued May 7, 1965; revised May 1, 1966; revised January 1968.

[6] A. G. Longley, "Radio Propagation in Urban Areas," Tech. Rep., OT Report, April 1978.

[7] R. Edwards and J. Durkin, "Computer Prediction of Service Area for VHF Mobile Radio Networks," *Proceedings of the IEE*, vol. 116, no. 9, pp. 1493–1500, 1969.

[8] C. E. Dadson, J. Durkin, and E. Martin, "Computer Prediction of Field Strength in the Planning of Radio Systems," *IEEE Transactions on Vehicular Technology*, vol. VT-24, no. 1, pp. 1–7, February 1975.

[9] T. Okumura, E. Ohmori, and K. Fukuda, "Field Strength and Its Variability in VHF and UHF Land Mobile Service," *Review Electrical Communications Laboratory*, vol. 16, no. 9–10, pp. 2935–2971, September–October 1968.

[10] M. Hata, "Empirical Formula for Propagation Loss in Land Mobile Radio Services," *IEEE Transactions on Vehicular Technology*, vol. VT-29, no. 3, pp. 317–325, August 1980.

[11] European Cooperation in the Field of Scientific and Technical Research EURO-COST 231, "Urban Transmission Loss Models for Mobile Radio in the 900 and 1800 MHz Bands," Tech. Rep., The Hague, September 1991.

[12] J. Walfisch and H. L. Bertoni, "A Theoretical Model of UHF Propagation in Urban Environments," *IEEE Transactions on Antennas and Propagation*, vol. AP-36, pp. 1788–1796, October 1988.

[13] M. J. Feuerstein, K. L. Blackard, T. S. Rappaport, S. Y. Seidel, and H. H. Xia, "Path Loss, Delay Spread, and Outage Models as Functions of Antenna Height for Microcellular System Design," *IEEE Transactions on Vehicular Technology*, vol. 43, no. 3, pp. 487–498, August 1994.

[14] R. Skidmore, T. Rappaport, and A. Abbott, "Interactive Coverage Regions and Design Simulation for Wireless Communication Systems in Multifloored Indoor Environments: SMT *plus*," in *Proceedings of the* 5^{th} *IEEE International Conference on Universal Personal Communications*, Cambridge, 1996, pp. 646–650.

[15] T. S. Rappaport and S. Sandhu, "Radio Wave Propagation For Emerging Wireless Personal Communication Systems," *IEEE Antennas and Propagation Magazine*, vol. 136, no. 5, October 1994.

[16] A. M. D. Turkmani, J. D. Parson, and D. G. Lewis, "Radio Propagation into Buildings at 441, 900, and 1400 MHz," in *Proceedings of the Fourth International Conference on Land Mobile Radio*, December 1987.

[17] A. M. D. Turkmani and A. F. Toledo, "Propagation into and within Buildings at 900, 1800, and 2300 MHz," in *IEEE Vehicular Technology Conference*, 1992.

[18] E. H. Walker, "Penetration of Radio Signals into Buildings in Cellular Radio Environments," in *IEEE Vehicular Technology Conference*, 1992.

[19] J. M. Durante, "Building Penetration Loss at 900 MHz," in *IEEE Vehicular Technology Conference*, 1973.

[20] J. Horikishi et al., "1.2 GHz Band Wave Propagation Measurements in Concrete Buildings for Indoor Wireless Communications," *IEEE Transactions on Vehicular Technology*, vol. VT-35, no. 4, 1986.

[21] T. S. Rappaport et al., "Statistical Channel Impulse Models for Factory and Open Plan Building Radio Communication System Design," *IEEE Transactions on Communications*, vol. COM-39, no. 5, pp. 794–806, May 1991.

[22] T. S. Rappaport, W. Huang, and M. J. Feuerstein, "Performance of Decision Feedback Equalizers in Simulated Urban and Indoor Radio Channels," *IEICE Transactions on Communications*, vol. E76-B, no. 2, pp. 1993, February 1993.

[23] D. C. Cox and R. P. Leck, "Distributions of Multipath Delay Spread and Average Excess Delay for 910 MHz Urban Mobile Radio Paths," *IEEE Transactions on Antennas and Propagation*, vol. AP-23, no. 5, pp. 206–213, March 1975.

[24] T. S. Rappaport, S. Y. Seidel, and R. Singh, "900 MHz Multipath Propagation Measurements for U.S. Digital Cellular Radiotelephone," *IEEE Transactions on Vehicular Technology*, pp. 132–139, May 1990.

[25] A. A. M. Saleh and R. A. Valenzula, "A Statistical Model for Indoor Multipath Propagation," *IEEE Journal on Selected Areas in Communication*, vol. JSAC-5, no. 2, pp. 128–137, February 1987.

[26] D. J. Devasirvatham, M. J. Krain, and D. A. Rappaport, "Radio Propagation Measurements at 850 MHz, 1.7 GHz, and 4.0 GHz Inside Two Dissimilar Office Buildings," *Electronics Letters*, vol. 26, no. 7, November 1990.

[27] S. Y. Seidel et al., "The Impact of Surrounding Buildings on Propagation for In-Building Personal Communications System Design," in *1992 IEEE Vehicular Technology Conference*, Denver, May 1992, pp. 814–818.

[28] W. C. Y. Lee, *Mobile Cellular Telecommunications Systems*, McGraw-Hill, New York, 1989.

[29] J. Chuang, "The Effects of Time Delay Spread on Portable Communications Channels with Digital Modulation," *IEEE Journal on Selected Areas in Communications*, vol. SAC-5, no. 5, pp. 879–889, June 1987.

[30] Bernard Glance and Larry J. Greenstein, "Frequency-Selective Fading Effects in Digital Mobile Radio with Diversity Combining," *IEEE Transactions on Communications*, vol. COM-31, no. 9, September 1983.

[31] Victor Fung, Theodore Rappaport, and Berthold Thoma, "Bit Error Simulation for $\pi/4$ DQPSK Mobile Radio Communications using Two-Ray and Measurement-Based Impulse Response Models," *IEEE Journal on Selected Areas in Communications*, vol. 11, no. 3, April 1993.

[32] R. H. Clarke, "A Statistical Theory of Mobile-Radio Reception," *Bell Systems Technical Journal*, vol. 47, pp. 957–1000, 1968.

[33] M. J. Gans, "A Power Spectral Theory of Propagation in the Mobile Radio Environment," *IEEE Transactions on Vehicular Technology*, vol. VT-21, pp. 27–38, February 1972.

[34] J. C. Liberti and T. S. Rappaport, "A Geometrically Based Model for Line-of-Sight Multipath Radio Channels," in *1996 IEEE* 46^{th} *Vehicular Technology Conference*, Atlanta, May 1996, pp. 844–848.

[35] P. Petrus, J. H. Reed, and T. S. Rappaport, "Geometrically Based Statistical Macrocell Channel Model for Mobile Environments," in *IEEE Global Telecommunications Conference*, London, November 1996, pp. 1197–1201.

[36] T. Manabe, Y. Miura, and T. Ihara, "Effects of Antenna Directivity and Polarization on Indoor Multipath Propagation Characteristics at 60 GHz," *IEEE Journal on Selected Areas in Communications*, vol. 14, no. 3, pp. 441–448, April 1996.

[37] L. Talbi and G. Delisle, "Experimental Characterization of EHF Multipath Indoor Radio Channels," *IEEE Journal on Selected Areas in Communications*, vol. 14, no. 3, pp. 431–440, April 1996.

[38] T. Manabe et al., "Polarization Dependence of Multipath Propagation and High-Speed Transmission Characteristics of Indoor Millimeter-Wave Channel at 60 GHz," *IEEE Trans. on Vehic. Technol.*, vol. 44, no. 2, pp. 268–274, May 1995.

[39] R. Davies, M. Bensebti, M. Beach, and J. McGeehan, "Wireless Propagation Measurements in Indoor Multipath Environments at 1.7 GHz and 60 GHz for Small Cell Systems," in *Proceedings of the* 41^{st} *IEEE Vehicular Technologies Conference*, St. Louis, 1991, pp. 589–593.

[40] P. F. M. Smulders and A. G. Wagemans, "Wideband Indoor Radio Propagation Measurements at 58 GHz," *Electronics Letters*, vol. 28, no. 13, pp. 1270–1272, 1992.

[41] T. S. Bird et al., "Millimeter-Wave Antenna and Propagation Studies for Indoor Wireless LAN's," in *1994 IEEE Antennas and Propagation Society Symposium*, Seattle, June 19–24 1994, pp. 336–339.

[42] T. Manabe and T. Ihara, "Propagation Studies at 60 GHz for Millimeter-Wave Indoor Communications Systems," *J. Commun. Res. Lab.*, vol. 41, no. 3, pp. 167–174, November 1994.

[43] K. Sato et al., "Measurements of Reflection Characteristics and Refractive Indices of Interior Construction Materials in Millimeter-Wave Bands," in *Proc.* 45^{th} *IEEE Veh. Technol. Conf.*, Chicago, July 26–28 1995.

[44] A. R. Tharek and J. P. McGeehan, "Indoor Propagation and Bit Error Rate Measurements at 60 GHz using Phase-Locked Oscillators," in *Proc.* 38^{th} *IEEE Veh. Technol. Conf.*, May 1988, pp. 127–133.

[45] P. Smulders and A. Wagemans, "Wideband Measurements of mm-Wave Indoor Radio Channels," in 3^{rd} *IEEE Int. Symp. Personal Indoor Mobile Radio Communications*, October 1992, pp. 329–333.

[46] G. Kalivas, M. El-Tanany, and S. Mahmoud, "Channel Characterization for Indoor Wireless Communications at 21.6 GHz and 37.2 GHz," in 2^{nd} *Int. Conf. on Universal Personal Commun.*, Ottawa, October 1993, pp. 626–630.

[47] L. Talbi and G. Y. Delisle, "Measurement Results of Indoor Radio Channel at 37.2 GHz," in *ANTEM Symposium*, Ottawa, August 1994, pp. 19–23.

[48] P. W. Huish and G. Pugliese, "A 60 GHz Radio System for Propagation Studies in Buildings," in 3^{rd} *Int. Conf. on Antennas and Propagation*, 1983, vol. 2, pp. 181–185.

[49] J. Ahern, G. Y. Delisle, and Y. Chalifour, "Indoor mm-Wave Propagation Measurement System," in *Canadian Conf. on Elec. and Comp. Eng.*, 1991, vol. 2, pp. 9.1.1–9.1.4.

[50] L. Talbi and G. Y. Delisle, "Wideband Propagation Measurements and Modeling at Millimeter Wave Frequencies," in *Proc. IEEE GLOBECOM '94*, San Francisco, December 1994, vol. 1, pp. 47–51.

[51] J.D. Parsons and J.G. Gardiner, "Mobile Communication Systems," Tech. Rep., Blackie and Son, Limited, Glasgow, 1989.

[52] Thomas Kailath Ayman F. Naguib, Arogyaswami Paulraj, "Capacity Improvement with Base-Station Antenna Arrays in Cellular CDMA.," AUGUST 1994.

[53] J.C.Liberti, *Analysis of CDMA Cellular Radio Systems Employing Adaptive Antennas*, Ph.D. thesis, Virginia Tech, Blacksburg, VA, September 1995.

[54] Theodore S.Rappaport Joseph . Liberti, "Analysis of CDMA Cellular Radio Systems Employing Adaptive Antennas in Multipath Environments," in *IEEE Veh. Tech. Conf.*, Atlanta, GA, April 28-May 1 1996.